

MODELING OF AVALANCHES IN GRANULAR MEDIA

Lev S. Tsimring

Institute for Nonlinear Science, University of California, San Diego, La Jolla, CA
92093-0402

Igor S. Aranson

Argonne National Laboratory, 9700 South Cass Avenue, Argonne, IL 60439

ABSTRACT

We develop a continuum description of partially fluidized granular flows. Our theory is based on the viscoelastic equations for the flow coupled with the order parameter equation which describes the transition between flowing and static components of the granular system. This theory applies to many naturally occurring and technologically important phenomena: avalanches, shear flows, granular friction. In particular, it captures important phenomenology recently observed in experiments with granular flows on sticky inclined planes: bistability, transition from triangular avalanches propagating downhill at small inclination angles to balloon-shaped avalanches also propagating uphill for larger angles.

INTRODUCTION

Granular materials exhibit many unexpected phenomena which set them apart from conventional solids, liquids, and gases[1]. Because of the dissipative nature of the grain collisions, the dynamics of granular media requires constant supply of energy, making them essentially non-equilibrium systems. One of the most challenging theoretical tasks in understanding non-equilibrium granular dynamics is to develop a theory which is applicable both in solid and liquid phases of granular medium, and can describe phase transition between them. So far, the existing theoretical approaches included large-scale molecular dynamics simulations [2, 3] and two-phase models [4, 5, 6, 7]. In the two-phase continuum description, the granular system is spatially separated into two phases, static and rolling. The interaction between the phases is implemented through certain conversion rates. This model described certain features of thin near-surface granular flows including avalanches. However, due to its intrinsic assumptions, it only works when the granular material is well

separated in a thin surface flow and an immobile bulk. In many practically important situations, this distinction between “liquid” and “solid” phases is more subtle and itself is controlled by the dynamics. In this work we propose a unifying description of partially fluidized granular flows and apply this theory to several problems of granular dynamics.

We separate the shear stresses developing in a granular matter, in two parts: “static” (or strain-independent) part, and the dynamic part which proportional to the shear strain rate. The ratio between the dynamic and static parts of the shear stress is proportional to the order parameter (OP) which varies from 0 in the “liquid” phase to 1 in the “solid” phase. Unlike ordinary matter, the phase transition in granular matter is controlled not by the temperature, but the dynamics stresses themselves through a generalization of the Mohr-Coloumb yield criterion[8]. critical melting temperature of a solid. The OP can be related to the local entropy (and possibly density) [9] of the granular material. OP dynamics is then coupled to the hydrodynamic equation for the granular flow.

The most spectacular manifestation of the solid-liquid transition in granular media occurs during an avalanche. There has been a number of experimental studies of avalanche flows in large sandpiles[10, 11] as well as in thin layers of grains on sticky inclined surfaces [12, 13, 14].

We apply this model to study the transition to flow in thin granular layer on inclined planes with sticky bottom. Our model captures important phenomenology observed by Pouliquen[14] and Daerr and Douady[12], including the structure of the stability diagram, triangular shape of downhill avalanches at small inclination angles and balloon shape of uphill avalanches for larger angles.

GOVERNING EQUATIONS

The granular flow in the continuum limit can be described by the usual momentum conservation equation

$$\rho_0 \frac{Dv_i}{Dt} = \frac{\partial \sigma_{ij}}{\partial x_j} + \rho_0 g_i, \quad j = 1, 2, 3. \quad (1)$$

for three velocity components v_i . Here $\rho_0 = const$ is the material density (we set $\rho_0 = 1$), \mathbf{g} is gravity acceleration, and $D/Dt = \partial_t + v_i \partial_{x_i}$ is the material derivative. The velocity field also obeys the incompressibility condition $\nabla \cdot \mathbf{v} = 0$. As boundary conditions for the velocity field, we require the no slip $v_i = 0$ on solid walls, and the continuity $\frac{D\xi}{Dt} = v_n$ on free surfaces (here ξ is the displacement of the free surface, and v_n is the normal velocity component).

The crux of our model is that the stress tensor σ_{ij} can be expressed as a sum of the hydrodynamic part proportional to the flow strain rate e_{ij} , and the strain-independent part, σ_{ij}^s , i.e. $\sigma_{ij} = e_{ij} + \sigma_{ij}^s$. We assume that the diagonal elements of the static tensor σ_{ii}^s coincide with the corresponding components of the “true” static stress tensor σ_{ii}^0 for the immobile grain configuration in the same geometry, whereas the off-diagonal (shear) components of stress are reduced by the value of the order parameter ρ characterizing the

“phase state” of granular matter. Thus, we write the stress tensor in the form

$$\begin{aligned}\sigma_{ij} &= \eta \left(\frac{\partial v_i}{\partial x_j} + \frac{\partial v_j}{\partial x_i} \right) + \rho \sigma_{ij}^0, \quad i \neq j \\ \sigma_{ii} &= 2\eta \frac{\partial v_i}{\partial x_i} + \sigma_{ii}^0,\end{aligned}\tag{2}$$

where η is the normal viscosity coefficient. In a static state, $\rho = 1$, $\sigma_{ij} = \sigma_{ij}^0$, $v_i = 0$, whereas in a fully fluidized state $\rho = 0$, and the shear stresses are simply proportional to the strain rates as in ordinary fluids.

We assume that the order parameter dynamics is described by the variational equation $\dot{\rho} = -\delta\mathcal{F}/\delta\rho$. The “free-energy” functional \mathcal{F} has the standard Landau form $\mathcal{F} \sim \int \mathbf{dr} (D|\nabla\rho|^2 + f(\rho))$, so the order parameter equation reads

$$\dot{\rho} = D\nabla^2\rho - F(\rho)\tag{3}$$

where $F(\rho) = df(\rho)/d\rho$. The potential energy $f(\rho)$ should have extrema at $\rho = 0$ and $\rho = 1$ corresponding to uniform solid and liquid phases. According to the Mohr-Coulomb yield criterion for non-cohesive grains[8] or its generalization [15], the transition to flow occurs when the non-dimensional ratio $\phi = \max |\sigma_{mn}^0/\sigma_{nn}^0|$ exceeds a certain threshold value. In this expression, the maximum is sought over all possible orthogonal directions n and m in the bulk of the granular material. We use this ratio as a control parameter in the free energy density $f(\rho, \phi)$. Further, according to observations there is a range of stresses in which both static and dynamics phases co-exist (Bagnold hysteresis[10]). Correspondingly, in the range $\phi_0 < \phi < \phi_1$ free energy should have two minima at $\rho = 0, 1$. The simplest form of $F(\rho, \phi)$ which satisfies this condition, is $F(\rho, \phi) = a\rho(1 - \rho)(-\rho + \delta)$, where $\delta = (\phi - \phi_0)/(\phi_1 - \phi_0)$. Setting $D = 1$ and $a = 1$ we arrive at

$$\dot{\rho} = \nabla^2\rho + \rho(1 - \rho)(\rho - \delta).\tag{4}$$

For $\phi_0 < \phi < \phi_1$ both static ($\rho = 1$) and dynamic ($\rho = 0$) phases are linearly stable, and Eq.(4) possesses a moving front solution which “connects” these phases. The speed of the front in the direction of $\rho = 0$ is given by $V = (1 - 2\delta)/\sqrt{2}$.

CHUTE FLOW

In this section we analyze the stability properties of the granular flow in a shallow chute within the model (1),(2),(4). Consider a layer of dry cohesionless grains on an inclined sticky surface (see Fig.1) with slope $\tan\varphi$. According to Eq.(1), in the static equilibrium the following conditions should be satisfied:

$$\sigma_{zz,z}^0 + \sigma_{xz,x}^0 = -g \cos\varphi, \quad \sigma_{xz,z}^0 + \sigma_{xx,x}^0 = g \sin\varphi\tag{5}$$

where the subscripts after commas mean partial derivatives. The solution to Eqs. (5) in the absence of lateral stresses $\sigma_{yy}^0 = \sigma_{yx}^0 = \sigma_{yz}^0 = 0$, is given by

$$\sigma_{zz}^0 = -g \cos\varphi z, \quad \sigma_{xz}^0 = g \sin\varphi z, \quad \sigma_{xx,x}^0 = 0\tag{6}$$

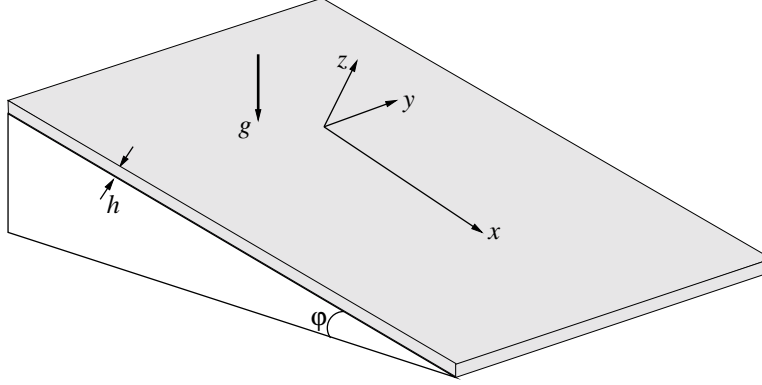


Figure 1: Schematic representation of a chute geometry

In a static equilibrium there is a simple relation between shear and normal stresses, $\sigma_{xz}^0 = -\tan \varphi \sigma_{zz}^0$. According to our model, this relation between the static components of the stress is maintained in the flowing regime as well. For the chute flow geometry, the most “unstable” yield direction is parallel to the inclined plane, so $\phi = |\sigma_{xz}^0/\sigma_{zz}^0|$.

Stationary solutions of Eq. (4) for the vertically confined chute geometry Fig. 1 are subject to the no-flux condition $\rho_z = 0$ at the free surface $z = 0$, and condition $\rho = 1$ at the bottom of the chute $z = -h$ (a granular medium is assumed to be in a solid phase near the sticky surface). There always exists a stationary solution to Eq. (4) $\rho = 1$ corresponding to a static equilibrium. For $\delta > 1$ it is stable at small h , but loses stability at a certain threshold $h_c > 1$. The most “dangerous” mode of instability satisfying the above boundary conditions, is $a \cos(\pi z/2h)$. The eigenvalue of this mode is $\lambda(h) = \delta - 1 - \pi^2/4h^2$, hence the neutral curve $\lambda = 0$ for the linear stability of the solution $\rho = 1$ is given by

$$h_c = \frac{\pi}{2\sqrt{\delta - 1}}. \quad (7)$$

For $h > h_c(\delta)$ grains spontaneously start to roll, and a granular flow ensues. In addition to the trivial state $\rho = 1$, for $h > h_s(\delta)$ there exists a unique non-trivial stationary solution satisfying the above boundary conditions. The value of h_s can be found as a minimum of the following integral as a function of ρ_0 , the value of ρ at the surface $z = 0$,

$$h_s = \min_{\rho_0} \int_{\rho_0}^1 \frac{d\rho}{\sqrt{\frac{\rho^4}{2} - \frac{2(\delta+1)\rho^3}{3} + \delta\rho^2 - c(\rho_0)}}, \quad (8)$$

where $c(\rho_0) = \rho_0^4/2 - 2(\delta + 1)\rho_0^3/3 + \delta\rho_0^2$. This integral can be calculated analytically for $\delta \rightarrow \infty$ and $\delta \rightarrow 1/2$. It is easy to show that for large δ , the critical solution of Eq.(4) has a form $\rho = 1 + a \cos(kz)$ with $a \ll 1$ and $k = (\delta - 1)^{1/2}$, and therefore, $h_s(\delta) \rightarrow h_c(\delta)$. For $\delta \rightarrow 1/2$, the critical phase trajectory comes close to two saddle points $\rho = 0$ and $\rho = 1$, and an asymptotic evaluation of (8) gives $h_s = -\sqrt{2} \log(\delta - 1/2) + const$. This expression agrees with the empirical formula $\phi - \phi_0 \sim \exp[-h_s/h_0]$ proposed in Ref. [12].

The neutral stability curve $h_c(\delta)$ and the critical line $h_s(\delta)$ limiting the region of existence of non-trivial granular flow solutions are shown in Fig.2 as solid and long-dashed line,

respectively. They divide the parameter plane (δ, h) in three regions. At $h < h_s(\delta)$, the trivial static equilibrium $\rho = 1$ is the only stationary solution of Eq.(4) for chosen BC. For $h_s(\delta) < h < h_c(\delta)$, there is a bistable regime, the static equilibrium state co-exists with the stationary flow. For $h > h_c(\delta)$, the static regime is linearly unstable, and the only stable regime corresponds to the granular flow. This qualitative picture completely agrees with the recent experimental findings[12, 14]. Moreover, if we rescale the experimental phase diagram obtained by Daerr and Dauady[12] using their asymptotic values $\phi_{0,1}$ for deep layers, and choose the characteristic length scale l to be equal to the particle size, we obtain and excellent agreement with our theoretical phase diagram (see Fig.2).

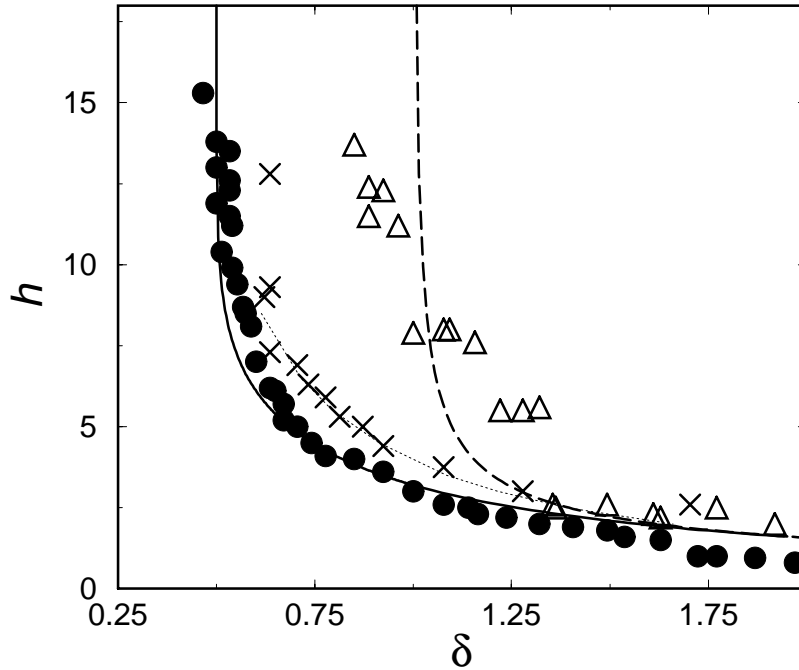


Figure 2: Stability diagram. Dashed line shows the neutral curve (7), solid line shows the existence limit of fluidized state (8), dotted line shows the transition from triangular to up-hill avalanches for $\beta = 3.15$ and $\alpha = 0.025$. Symbols show experimental data from Ref. [12].

The velocity profile corresponding to a stationary profile of $\rho(z)$, can be easily found from Eq. (2),

$$\eta \frac{\partial v_x}{\partial z} = g \sin \varphi z - \rho \sigma_{xz}^0 = g \sin \varphi (1 - \rho) z. \quad (9)$$

The flux of grains in the stationary flow J is given by

$$J = \int_{-h}^0 v_y(z) dz = \frac{g \sin \varphi}{\eta} \int_{-h}^0 \int_{-h}^z (1 - \rho(z')) z' dz' dz \quad (10)$$

Pouliquen [14] proposed a scaling for the mean velocity $\bar{v} = J/h$ vs thickness of the layer h in the stationary flow regime, $\bar{v} \propto h^{3/2}/h_s$, which works for angles φ as well as for different grain sizes. Eq. (10) yields $v \propto (h - h_s)^{1/2}$ for small $h - h_s$ and $v \propto h^2$ for large h . It is plausible that the experimentally found scaling exponent 3/2 is the result of the crossover between two different regimes. However, renormalization \bar{v}/\sqrt{gh} , h/h_s as in Ref.[14] does not collapse our results onto a single curve, perhaps due to the assumption of a simple Newtonian relation between the strain v_z and the hydrodynamic part of the shear stress σ_{xz} with a fixed viscosity η (see Eq.(2)). In fact, η itself may depend on ρ and z in some fashion.

For a deep chute ($h \gg 1$), the stationary solution of Eq.(4) can be found analytically (cf. Ref.[16]). However, in this case the slope of the free surface may not be equal to the slope of the inclined plane, but is itself determined by the amount of sand which is poured on the surface up-stream. Thus, the closure of the problem will be provided by the constraint $J = \text{const}$.

AVALANCHES IN A SHALLOW CHUTE

In this section we consider non-stationary solutions of the shallow chute model which describe the onset of an avalanche. For a shallow chute, we can use Galerkin expansion in the direction transversal to the inclined plane, and in the first order look for solution in the form

$$\rho = 1 - A \cos\left(\frac{\pi}{2h}z\right) + \text{h.o.t.}, \quad (11)$$

where $A \ll 1$ is a slowly varying function of t , x , and y . Substituting ansatz (11) into Eq. (3) and applying orthogonality conditions, we obtain

$$A_t = \lambda(h)A + \nabla_{\perp}^2 A + \frac{8(2-\delta)}{3\pi}A^2 - \frac{3}{4}A^3 \quad (12)$$

where $\nabla_{\perp}^2 = \partial_x^2 + \partial_y^2$, $\lambda(h) = \delta - 1 - \frac{\pi^2}{4h^2}$. Deriving this equations we assumed that $(2-\delta)A^2$ and A^3 are of the same order, i.e. $\delta \approx 2$, however qualitatively similar equation with a different nonlinearity can be obtained for any δ and h . Eq. (12) must be coupled to the mass conservation equations which reads as (here we neglect contribution from the flux along y -axis $J_y \sim \partial_y h \ll J$):

$$\frac{\partial h}{\partial t} = -\frac{\partial J}{\partial x} = -\alpha \frac{\partial h^3 A}{\partial x}, \quad (13)$$

where J was calculated from Eq. (10) and $\alpha = 2(\pi^2 - 8)g \sin \varphi / \eta \pi^3$. Taking into account that variations in h also change local surface slope, we adopt $\delta = \delta_0 - \beta h_x$ with $\beta = 1/(\phi_1 - \phi_0)$.

We solved Eqs. (12),(13) numerically using finite difference method. The calculations were performed for large rectangular systems, typically 400 dimensionless units in x -direction (downhill), and 200 units in y -direction, with the number of grid points 1200×600 correspondingly. At $t < 0$, the layer was assumed static and uniform in thickness, $A =$

0, $h = h_0$. Avalanche is triggered by a localized perturbation introduced near the point $(y, z) = (L_y/4, L_z/2)$ at $t = 0$. Close to the solid line in Fig. (2) we observed avalanches propagating only downhill, with the shape very similar to the experimental one. The avalanche leaves triangular trace with the opening angle ψ in which the layer thickness h is decreased with respect to original value h_0 . At the front of the avalanche the layer depth is increased with respect to h , as in experiment. At any given point, the order parameter eventually returns to the “solid” value $\rho = 1$ which indicates the convective character of this avalanche.

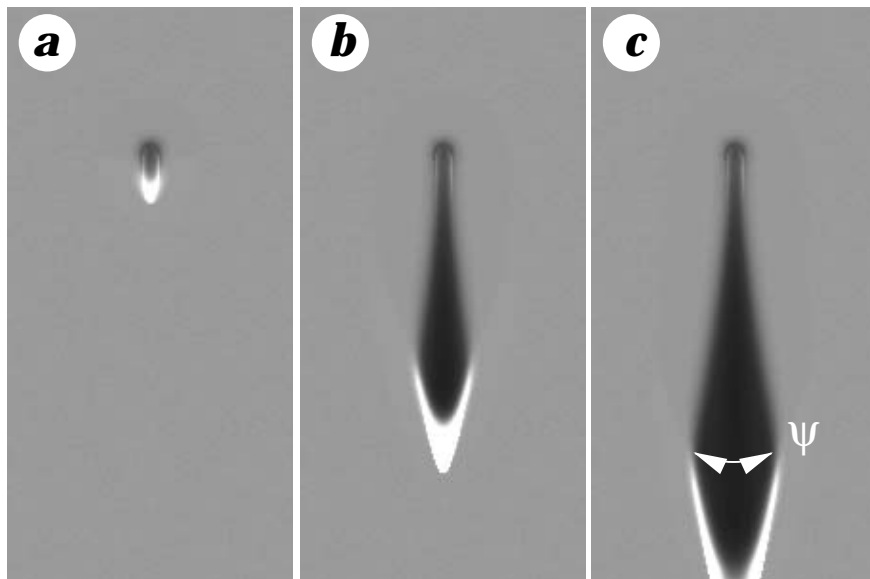


Figure 3: Development of triangular avalanche for $t = 50$ (a), $t = 200$ (b) and 250 (c). White shade correspond to maximum height of the layer, and black to minimum height. Parameters of Eqs. (12,13) are: $\alpha = 0.15, \beta = 0.25, \delta = 1.2$ and $h_0 = 3$, point A in Fig. 2.

For larger values of δ or layers thickness (close to dashed line in Fig. 2), the avalanche propagates also uphill, and contrary to the previous case, the avalanche zone is always in motion, as new rolling particles are constantly arrive from the upper boundary of the avalanche zone. Sometimes we observed small secondary avalanches in the wake of large primary avalanche, see Fig. 4c. This regime is analogous to the case of absolute instability.

CONCLUSIONS

In conclusion, we developed a continuum theory applicable to modeling of partially fluidized granular flows. We demonstrated that this theory captures important aspects of the phenomenology of chute flows observed in recent experiments [12, 13, 14], including the structure of the stability diagram, triangular shape of downhill avalanches at small inclination angles and balloon shape of uphill avalanches for larger angles.

We have also applied our model to the description flow in 2D rotating drum and of shear granular flows in Couette geometry, and found the experimentally observed features such

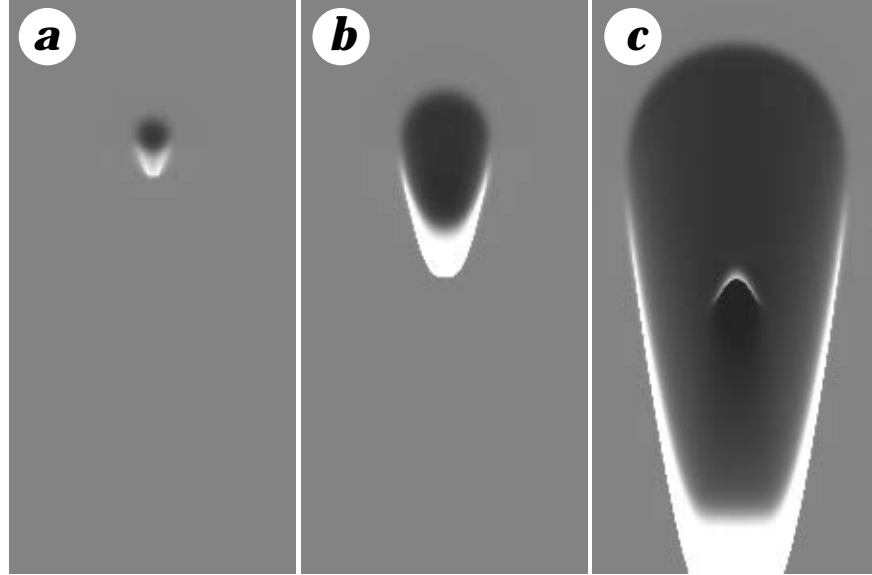


Figure 4: Development of up-hill avalanche for $t = 40$ (a), $t = 100$ (b) and 180 (c). Parameters of Eqs. (12,13) are: $\alpha = 0.05$, $\beta = 0.25$, $\delta = 1.07$ and $h_0 = 5.5$, point B in Fig. 2. A small secondary avalanche is seen on the image (c).

as periodic oscillations of the shear stress and flow velocity at low rotation rates (stick-slip) and transition to steady flow at higher rates. For shear cell experiment our model gives rise to the exponential velocity profile in two dimension and also deviation from exponential behavior in three dimensions. We believe that our modeling approach can be applicable to other granular flows and can be generalized on binary mixtures of granular materials.

ACKNOWLEDGEMENT

We thank Dan Howell, Deniz Ertas, Joe Goddard, Bob Behringer and Adrian Daerr for useful discussions. This research is supported by the Office of the Basic Energy Sciences at the US Department of Energy, grants DE-FG03-95ER14516 (L.T.) and W-31-109-ENG-3 (I.A.).

References

- [1] H.M. JAEGER, S.R. NAGEL, and R.P. BEHRINGER, *Physics Today* **49**, 32 (1996); *Rev. Mod. Phys.* **68**, 1259 (1996).
- [2] D. ERTAS et al, cond-mat/0005051.
- [3] O.R. WALTON, *Mech. Mater.* **16**, 239 (1993); T. Pöshel, *J. Phys. II France* **3**, 27 (1993); X.M. ZHENG and J.M. HILL, *Powder Tech.* **86**, 219 (1996); O. POULIQUEN and N. RENAUT, *J. Phys. II France* **6**, 923 (1993).

- [4] P.G. de GENNES, in *Powders & Grains*, R. Behringer & Jenkins (eds), p.3, Balkema, Rotterdam, 1997.
- [5] J.-P. BOUCHAUD, M.E. CATES, J. RAVI PRAKASH, and S.F. EDWARDS, *J. Phys. I France* **4**, 1383 (1994).
- [6] T. BOUTREUX, E. RAPHAËL, and P.G. de GENNES, *Phys. Rev. E* **58**, 4692 (1998).
- [7] T. BOUTREUX and E. RAPHAËL, *Phys. Rev. E* **58**, 7645 (1998).
- [8] R.M. NEDDERMAN, *Statics and Kinematics of Granular Materials*, (Cambridge University Press, Cambridge, England, 1992).
- [9] S.F. EDWARDS and R.B.S. OAKESHOTT, *Physica A* **157**, 1080 (1989); S. F. EDWARDS and D.V. GRINEV, *Chaos*, **9**, 551 (1999).
- [10] R.A. BAGNOLD, *Proc. Roy. Soc. London A* **225**, 49 (1954); *ibid.*, **295**, 219 (1966).
- [11] J. RAJCHENBACH, in *Physics of Dry Granular Media*, eds. H. Hermann, J.-P. Hovi, and S. Luding, p. 421, (Kluwer, Dordrecht, 1998); D. McClung, *Avalanche Handbook*, (Mountaineers, Seattle, 1993).
- [12] A. DAERR and S. DOUADY, *Nature (London)* **399**, 241 (1999).
- [13] A. DAERR, submitted to *Phys. Fluids*, 2000.
- [14] O. POULIQUEN, *Phys. Fluids*, **11**, 542 (1999).
- [15] M.E. CATES et al, *Phys. Rev. Lett.* **81**, 1841 (1998).
- [16] I. S. ARANSON, V.A. KALATSKY, and V.M. VINOKUR, *Phys. Rev. Lett.*, **85**, 118 (2000).